

Digital and Spatial Characterization of PD-L1 Expression and IVD Performance in the Immune Landscape of Head and Neck Squamous Cell Carcinoma: A Multimodal Approach

Clara I Troccoli, Lauren Matelski, Micaela Young, Huong Nguyen, Joseph Gibb, David Henderson, Adam Beharry, Vanessa Ly, Morgan Wambaugh, Melanie Amen, Will Paces, Geoff Metcalfe, Roberto Gianani, Tom Turi

Flagship Biosciences, Inc, 11800 Ridge Parkway Suite450, Broomfield, CO

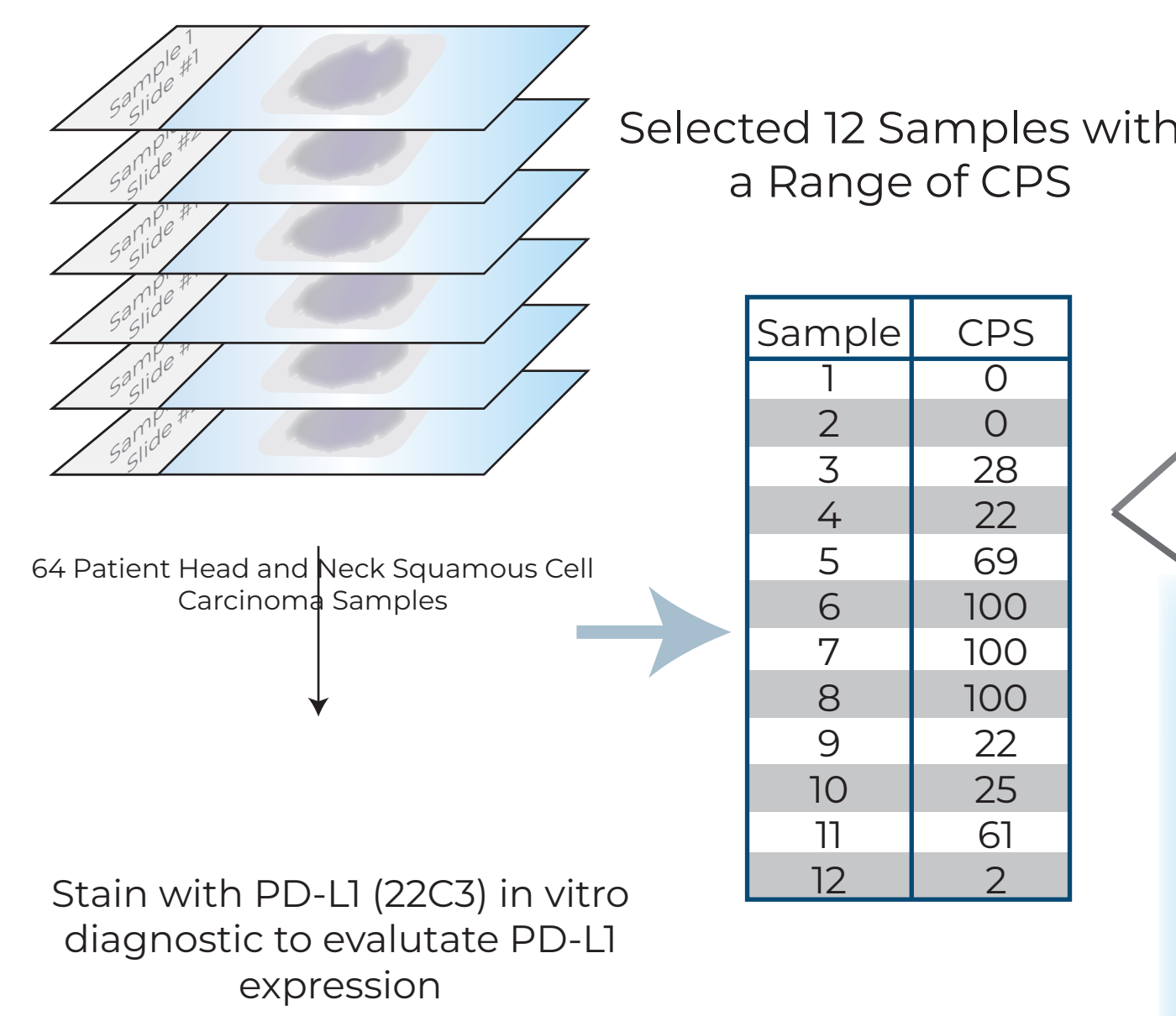


Abstract

The anti-PD-L1 antibody (22C3) is used as a companion diagnostic for successful checkpoint inhibitor therapy in head and neck squamous cell carcinoma. The positive predictive value of this assay, however, is less than ideal as a high PD-L1 score does not necessarily associate with a good response, and a good response may be seen with a low or negative PD-L1 score. In principle, this could be due to lack of accuracy and/or precision of the assay, as well as biological factors, such as variable expression across tumor cells and interacting immune cells. In this study, we describe a digital image analysis algorithm to address assay-related problems and improve both accuracy and precision, as well as improve identification of PD-L1 expression in differing cell populations of the tumor microenvironment. In addition, we propose a panel of assays that in aggregate might reveal inherent heterogeneity among cases with similar PD-L1 score and thus provide vital context underlying the efficacy of checkpoint inhibitors in the clinic. Here we show that applying novel machine-learning based digital image analysis to multiplex assays together with digital scoring of PD-L1 provides an accurate and precise assessment of the real-world tumor milieu that we hypothesize will help establish the immunophenotypes that inform therapeutic efficacy of checkpoint inhibitors. We have additionally interrogated whether expression of PD-L1 in these groups are consistent with known molecular patterns assayed using novel methodologies, such as high-plex digital spatial transcriptomics through the nanoString GeoMx Digital Spatial Profiler (DSP) platform and assessed the ability of the different digital platforms to provide concordant data relating to real-world expression patterns of PD-L1 and associated biomarkers. Thus, our results point to the importance of robust methodologies, used in combination, to evaluate complex tumor immune landscapes and the advantages of digital analyses to provide accurate and precise clinical contexts for better patient outcomes.

Multimodal Methodology

Evaluate Patient PD-L1 Status



CPS	Expression Level for FDA-Approved Therapy
< 1%	No Expression (No Therapy)
≥ 1%	Expression
≥ 50%	High Expression

Immunoprofiling of Each ROI With NanoString GeoMx® Digital Spatial Profiler Pathologist Established ROIs within Tumor Tissue

Inflamed Tumor	Tumor containing inflammatory cells.
Uninflamed Tumor	Tumor containing no inflammatory cells.
Excluded	Uninflamed tumor surrounded by stroma-containing inflammatory cells.

Multiplex Immunofluorescence (mIF) Staining Coupled with Flagship's Proprietary Image Analysis

CD86	Receptor involved in T-lymphocyte proliferation and IL-2 production.
CD206	Transmembrane protein predominantly expressed in tissue macrophages and dendritic cells.
CD64	Fc receptor on macrophages and monocytes and triggers cell activation under pro-inflammatory conditions.
CD163	Macrophage-specific protein upregulated expression involved in the switch to alternate activated phenotypes.
CD68	Localized to lysosomes and endosomes, functions to clear debris, promote phagocytosis, and mediate macrophage activation.

PD-L1 Expression

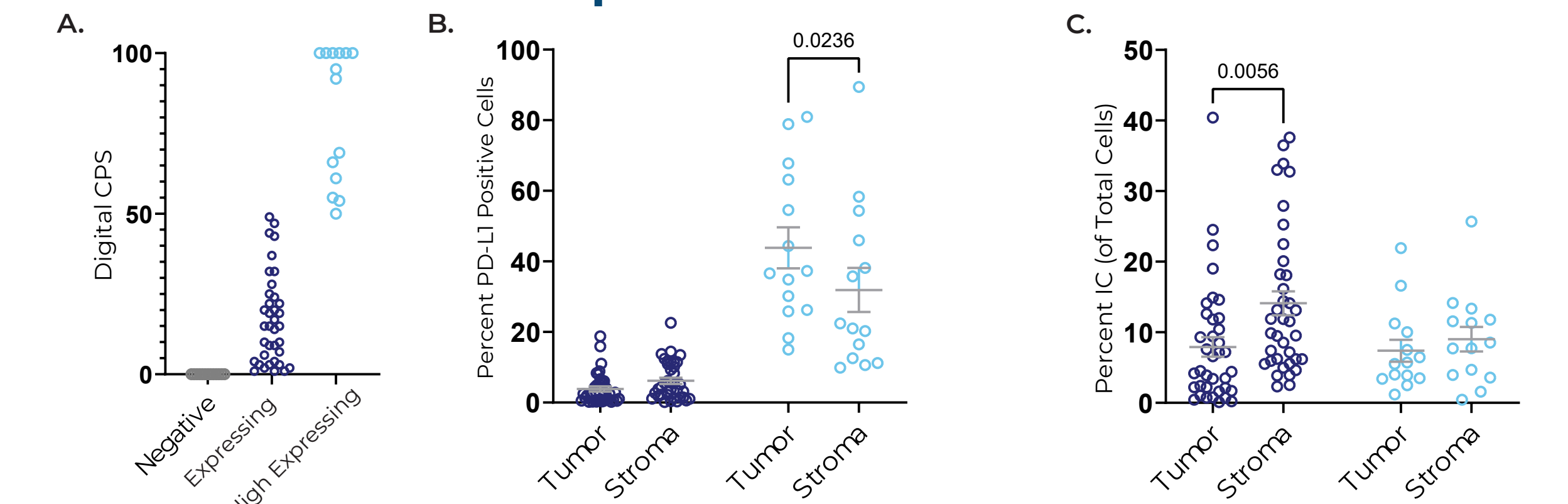


Figure 2. PD-L1 (22C3) Status with Flagship's Tumor/Stroma Separation. A) Distribution of CPS scores in patient samples analyzed for PD-L1 (22C3) staining. Note CPS is by convention capped at 100%. N=64 (13 Negative, 37 Expressing, 14 High Expressing). B) PD-L1 Expression (N=37) and High Expression (N=14) samples separated by tumor and stroma. Mean with SEM; 2way ANOVA with Bonferroni's multiple comparisons test. Main effect of PD-L1 status ($P < 0.0001$) and significant interaction ($P + 0.01$). C) PD-L1 Expression (N=37) and High Expression (N=14) Immune Cells (IC) (macrophages and/or lymphocytes) within the tumor and stroma compartments. Mean with SEM; 2way ANOVA with Bonferroni's multiple comparisons test. Main effect of compartment ($p=0.046$).

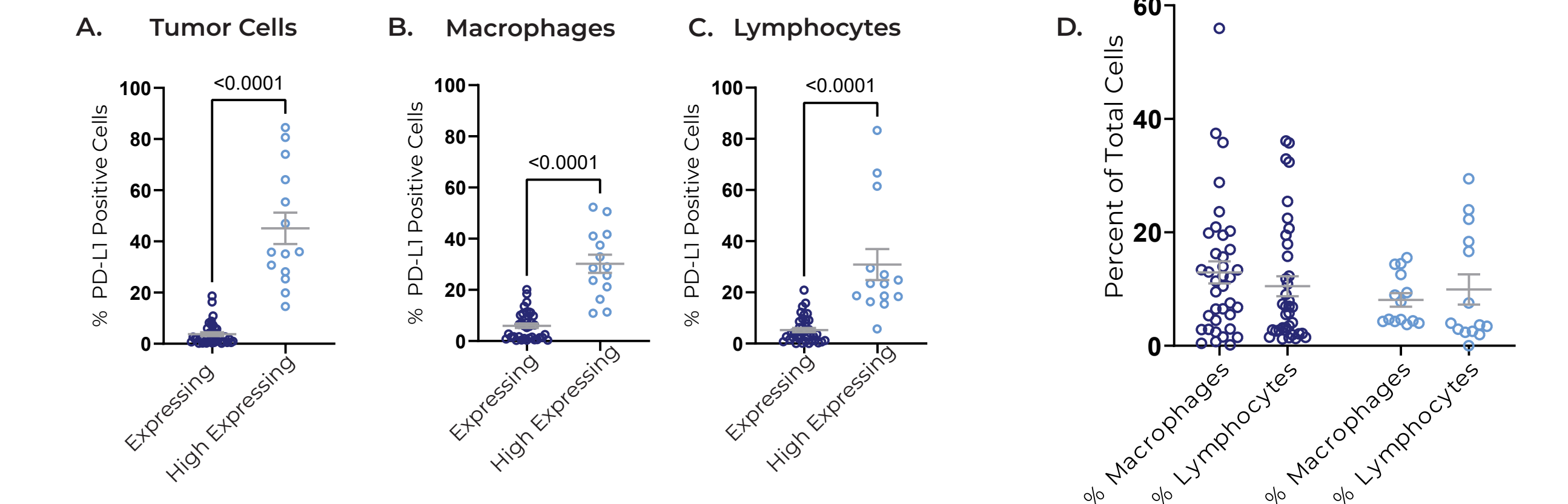
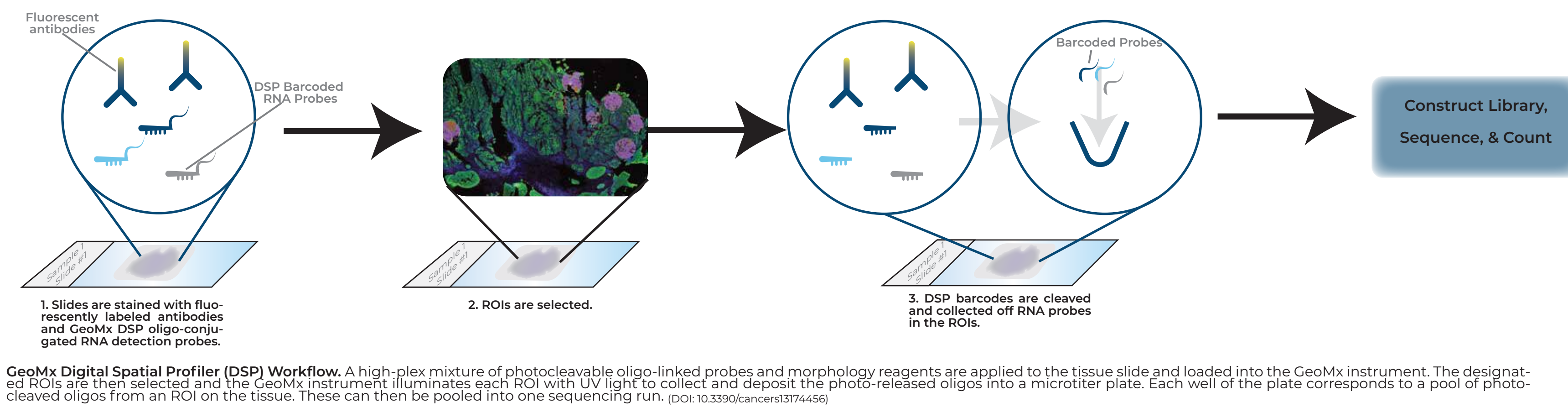


Figure 3. PD-L1 Expression and High Expressing Samples with Flagship's Cell Type Separation. A) PD-L1 Expression (N=37) and High Expressing (N=14) tumor cells. Mean with SEM; Mann-Whitney (nonparametric) test. B) PD-L1 Expression (N=37) and High Expressing (N=14) macrophages. Mean with SEM; Unpaired t-test with Welch's correction. C) PD-L1 Expression (N=37) and High Expressing (N=14) lymphocyte cells. Mean with SEM; Mann-Whitney (nonparametric) test. D) Percent of macrophages and lymphocytes in the whole tissue for PD-L1 Expression (N=37) and High Expressing (N=14) samples. Mean with SEM; 2way ANOVA with Bonferroni's multiple comparisons test (no significant main effect or multiple comparisons).

PD-L1 High Expressing samples contain increased PD-L1 expressing tumor cells but also macrophages and lymphocytes, though expressing and high expressing samples contain similar numbers of macrophages and lymphocytes.

GeoMx ROI Immunoprofiling



GeoMx Digital Spatial Profiler (DSP) Workflow. A high-plex mixture of photocleavable oligo-linked probes and morphology reagents are applied to the tissue slide and loaded into the GeoMx instrument. The designated ROIs are then selected and the GeoMx instrument illuminates each ROI with UV light to collect and deposit the photo-released oligos into a microtiter plate. Each well of the plate corresponds to a pool of photo-cleaved oligos from an ROI in the tissue. These can then be pooled into one sequencing run. (doi:10.3390/cancers1374456)

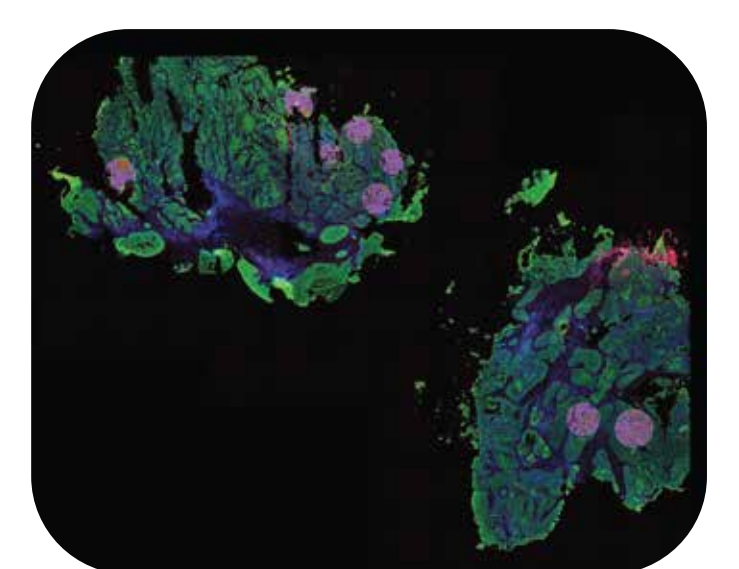


Figure 4. GeoMx ROIs for immunoprofiling. Purple circle represents an ROI used for analysis. ~75 ROIs were chosen across 12 patient samples.

Nanostring GeoMx Whole Transcriptome Atlas (WTA) Panel was utilized. Over 7800 genes were assessed per ROI.

Over 5600 genes were detected above background level.

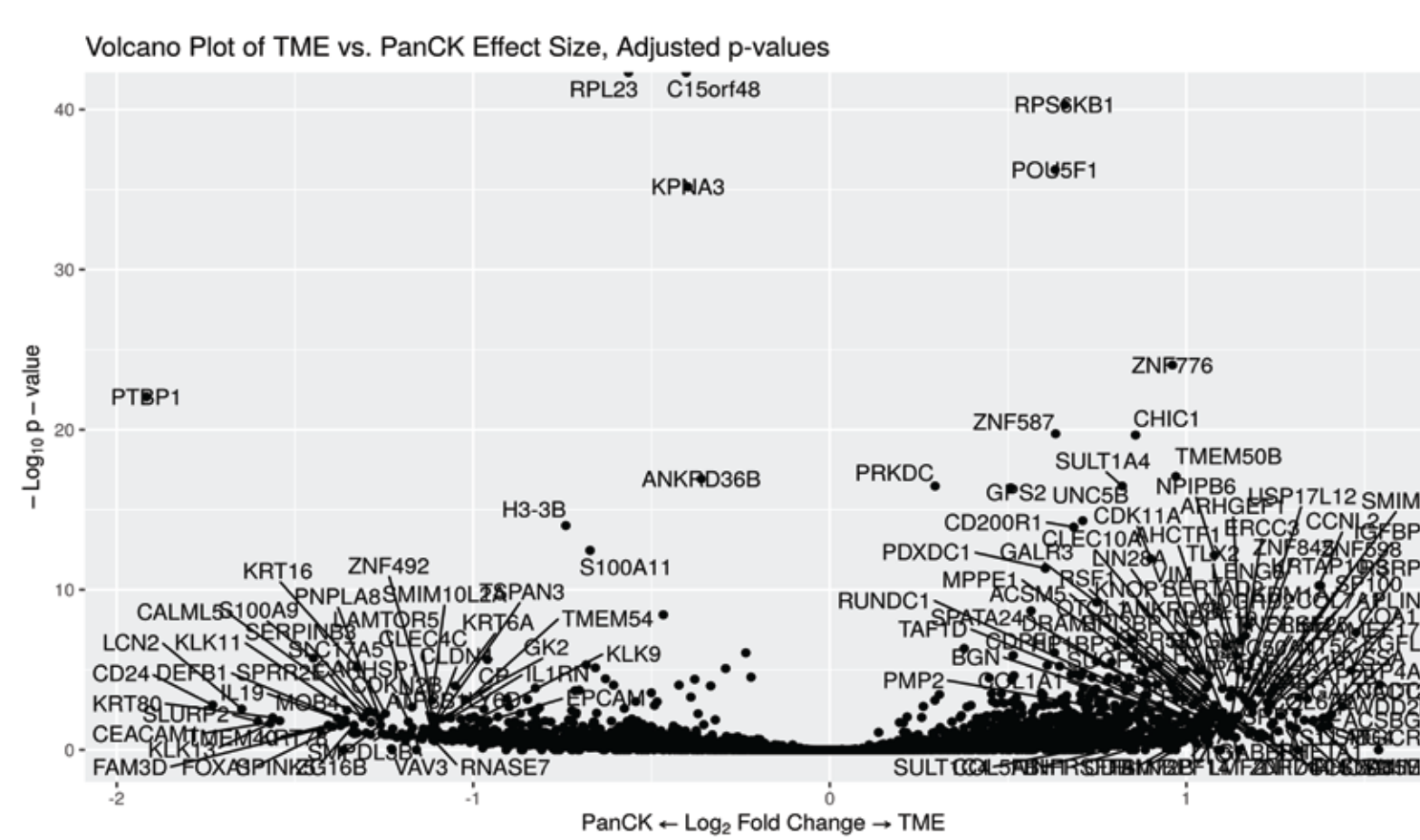


Figure 5. Volcano Plot of Highly Expressed Genes. Highly expressed genes from Tumor (PanCK) ROIs (left) versus Stroma (TME) ROIs (right).

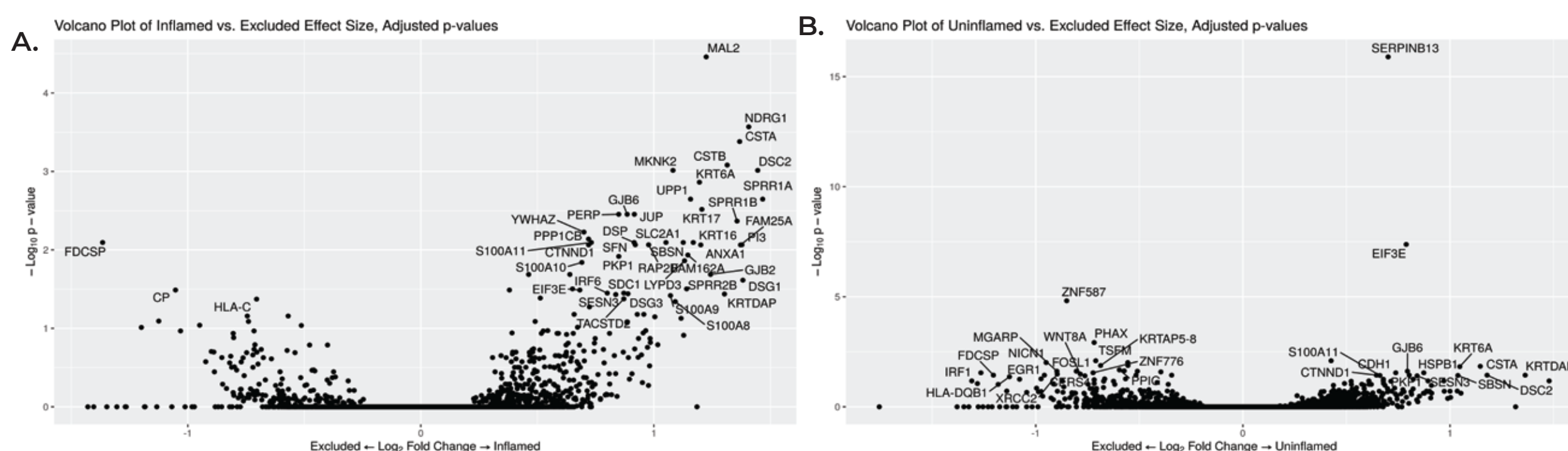


Figure 6. Volcano plots indicating highly expressed genes in comparisons. A) Inflamed ROIs (left) versus Excluded ROIs (right). B) Uninflamed ROIs (left) versus Excluded ROIs (right).

Multiplex Immunofluorescence and Image Analysis

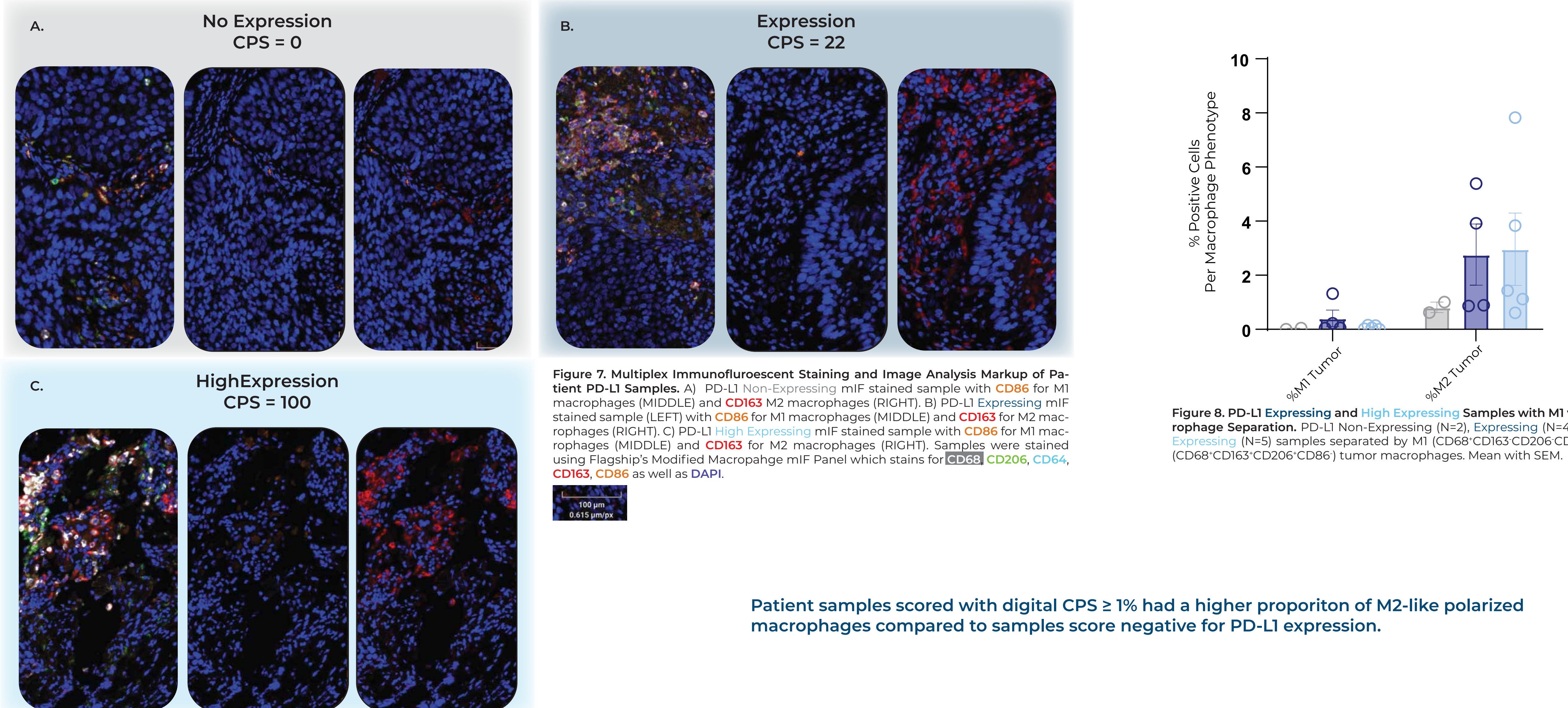


Figure 7. Multiplex Immunofluorescent Staining and Image Analysis Markup of Patient PD-L1 Samples. A) PD-L1 Non-Expressing mIF stained sample with CD86 for M1 macrophages (MIDDLE) and CD163 M2 macrophages (RIGHT). B) PD-L1 Expressing mIF stained sample (LEFT) with CD86 for M1 macrophages (MIDDLE) and CD163 for M2 macrophages (RIGHT). C) PD-L1 High Expressing mIF stained sample with CD86 for M1 macrophages (MIDDLE) and CD163 for M2 macrophages (RIGHT). Samples were stained using Flagship's Modified Macrophage mIF Panel which stains for CD68, CD206, CD64, CD163, CD86 as well as DAPI.

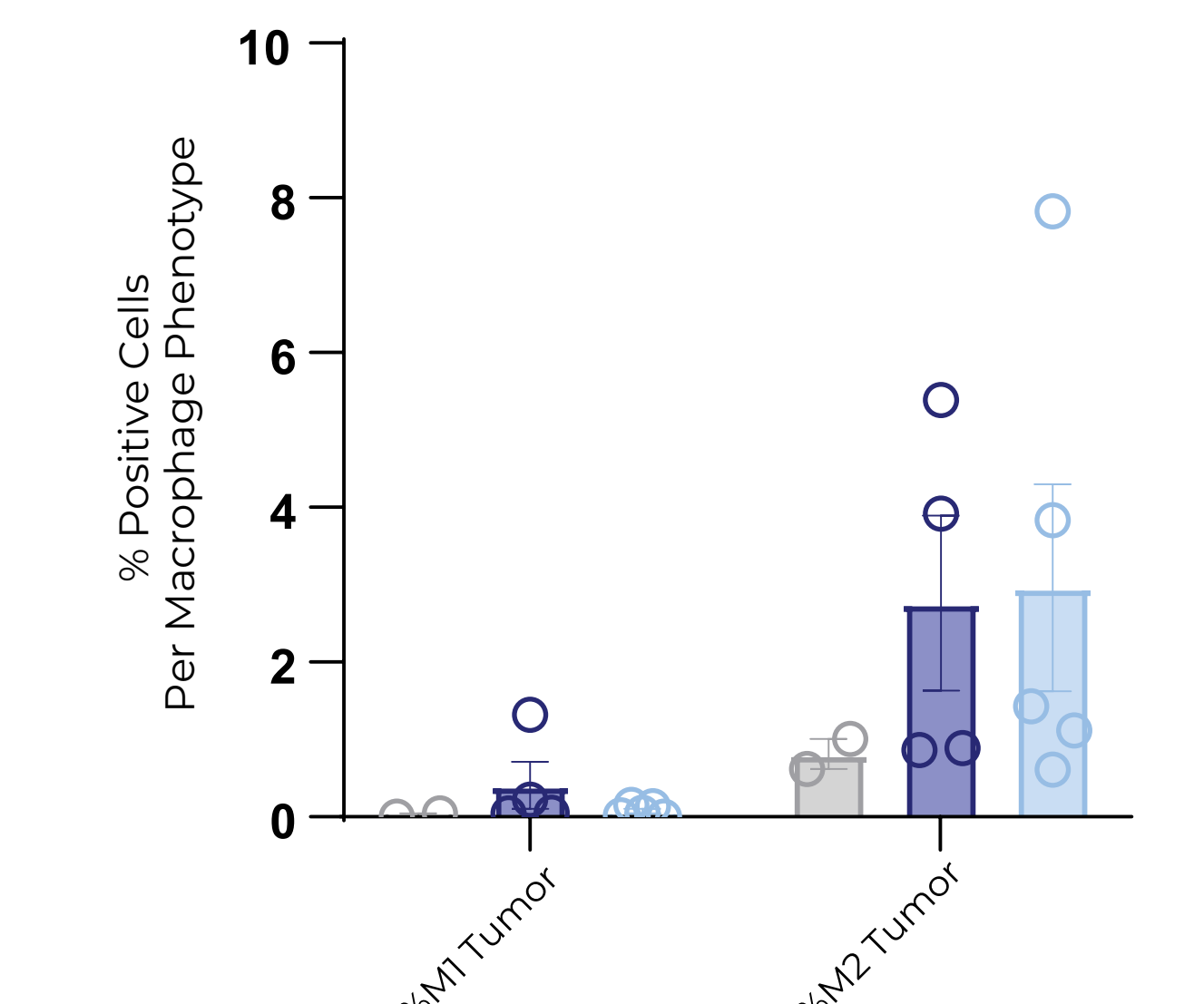


Figure 8. PD-L1 Expression and High Expressing Samples with M1 vs M2 Macrophage Separation. PD-L1 Non-Expressing (N=2), Expressing (N=4) and High Expressing (N=5) samples separated by M1 (CD68⁺CD163⁻CD206⁻CD86⁻) vs M2 (CD68⁻CD163⁺CD206⁺CD86⁺) tumor macrophages. Mean with SEM.

Patient samples scored with digital CPS $\geq 1\%$ had a higher proportion of M2-like polarized macrophages compared to samples score negative for PD-L1 expression.

Separating PD-L1 (22C3) Staining by Region (Tumor Vs. Stroma) or Cell Type (tumor, macrophage, lymphocyte) adds additional insight into the PD-L1 Status Landscape

Conducting Immunoprofiling on Specific ROIs yields insights into upregulated genes and pathways for each ROI.

Multiplex Immunofluorescence coupled with Tumor vs Stroma separations add insight to the types of macrophages within the tumor compartments.

Flagship's Proprietary Image Analysis coupled with Histology and Immunoprofiling Create a Comprehensive Characterization of the Immune Landscape of Head and Neck Squamous Cell Carcinoma Samples.